17

Investigation of the Unsteady Mechanism in the Generation of Propulsive Force While Swimming Using a Synchronized Flow Visualization and Motion Analysis System

Kazuo Matsuuchi and Yuki Muramatsu
University of Tsukuba
Japan

1. Introduction

The highly efficient locomotion of birds, insects and fish is based on unsteady dynamics. The central mechanism in their locomotion is related to the unsteady behaviour of vortices such as the formation and shedding of boundary layers developed on their bodies. The relation between an object and vortex movement was first noticed in the field of aeronautics. The problem of a thin aerofoil performing small lateral oscillations in a uniform stream of an incompressible fluid, which is at the heart of all flutter prediction, has received interest for many years. A great deal of research within the scope of the linear perturbation theory has been published in past times. Well-documented summaries can be seen in Bisplinghoff et al. (1955).

Recently, significant attention has been given to the lift-sustaining flight of insects and birds despite their weight, and many fruitful discoveries have been made. Flow unsteadiness was found to play an important role in the flights. However, the unsteady mechanism in swimming propulsion has received relatively little interest. The first important contribution related to the mechanism of propulsion in a swimming stroke was made by Counsilman (1971), who divided the force of a swimming stroke into two components: a lift component normal to the hand motion and a drag component parallel to it. He pointed out the greater importance of lift force rather than drag force. The next critical contribution was made by Schleihauf (1979), who measured the lift and drag forces on hand models for various geometrical configurations of flow. Berger et al. (1995) carried out similar measurements using hand and arm models in fixed geometrical configurations within a flow and obtained the results consistent with those of Schleihauf. Subsequently, Bixler and Riewald (2002) used a numerical approach under a scenario similar to the experiments described above. Each of the approaches mentioned above can be termed a *quasi-steady analysis*, which depends on the assumption that the flow at each instance is nearly steady.

Studies using flow visualisation have revealed the importance of a rotating water mass (Ungerechts (1981)), which focused attention on the contribution of vortices in propulsion.

Ungerechts (1986) also pointed out the importance of the turning phase of the leg kick during a breast stroke and found that the acceleration peak of the body is in approximate agreement with the turning phase of the feet. This observation suggests that vortices generated during this phase are related to the body force or its acceleration. Arellano (1999) investigated the vortices generated while swimming underwater, and showed that the size and the movement of the vortex seem to be related to the propulsion obtained through the hand and foot movements. Arellano et al. (2002) also described the difference between efficient and less efficient swimmers from the perspective of generated vortex patterns of vortices. Colwin (2002) provided several detailed sketches of vortices generated during various stroke patterns. Recently, a method approaching the unsteadiness has been actively developed by numerically solving the Navier-Stokes equations; however, its reliability is somewhat poor and there are many cases in which the experimental validation is needed.

The only method for analyzing quantitatively an unsteady flow is particle image velocimetry (PIV). This method is used to determine the displacement of particles dispersed in water within a short time interval. This method was successfully used in the fields of insect and fish locomotion. Even with the use of this sophisticated method, however, it is difficult to measure an entire flow field directly around a human hand and foot. Using PIV Matsuuchi et al. (2004) first demonstrated the flow field occurring around a moving hand while swimming, which may be the main source of propulsion for the crawl stroke. Momentum generation was estimated from this flow field obtained through PIV (Matsuuchi et al. (2009). According to Newton's second law of motion, the increment of momentum leads directly to the force generation. A remarkable amount of momentum was found to be produced in the transition phase from an in-sweep to out-sweep motion during a crawl stroke.

However, since the hand motion and flow field were measured separately, or independently, our knowledge on the instance when the vortices of coherent structure are generated was limited. To determine the mechanism on force generation in more detail, we have developed a new PIV system combined with the motion analysis, called SMAP (**S**ynchronized System of **M**otion **A**nalysis and **P**IV). This system is synchronized with the direct linear transformation (DLT) method for motion analysis. In the motion analysis we used two high-speed cameras which are available to a 3D analysis. The system can measure the flow fields, i.e., velocity and vorticity fields and the geometrical configuration of hand simultaneously.

2. Importance of unsteady behavior

It is well known that the unsteady mechanism plays a crucial role in the the generation of propulsive force in birds, insects and fish (for example, see Dickinson(1996)). In most cases vortex behaviors such as formation and shedding are important.

Before introducing our system and its results, we illustrate the importance of unsteadiness using an example of a flow field around a human hand. First we show an example of velocity field in a horizontal plane around a hand during a crowl stroke (see Fig. 1). The subject is a female Olympic swimmer in a flume set at a velocity 1.5 m/s. She swims from right to left. The generation of momentum can be seen in the direction opposite to her swimming direction, i.e., from the left to right. It is easy to see that the momentum is

generated between a pair of vortices. This generation of momentum leads directly to the propulsive force in swimming. In the figure, the mean velocity averaged over the entire plane has already been subtracted from the real velocity. This subtraction was made to emphasize the deviation from the mean velocity. The asterisk in the figure marks the location of the tip of the middle finger. Next in Fig. 2 we pick up an image file from which the Fig. 1 is drawn. This figure also shows the locations of the swimmer's hand 1/15 s before and after the instant the image was taken, which are depicted by cross marks. In addition to these locations, a predicted trace of the finger is depicted by a dotted line.

From the figure it is easy to see that two problems arise. One problem is the uncertainty of the finger positions and also the hand orientation. This problem is fatal, as a detailed hand orientation is important to determine the unsteady mechanism of force production. The other problem is that the 1/15 s interval of two subsequent events is too long to know the precise variation of a hand motion. The latter problem is very difficult to overcome, as shorter intervals are difficult to choose in a usual PIV system. However, the former problem is easily resolved by appying motion analysis with a high-speed camera, as will be mentioned in the next section.

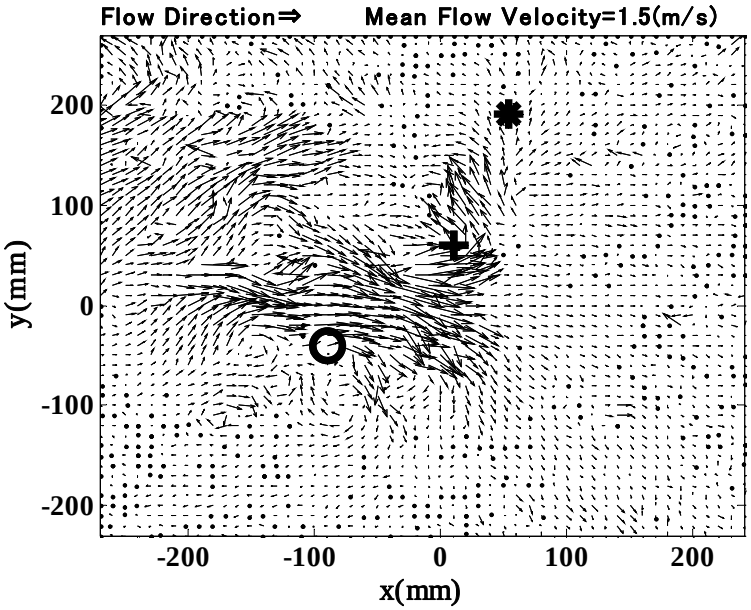

Fig. 1. Velocity field near a hand position, the third finger of which is located at the position shown by the asterisk. The cross mark and open circle denote the locations of vortices rotating anticlockwise and clockwise, respectively.

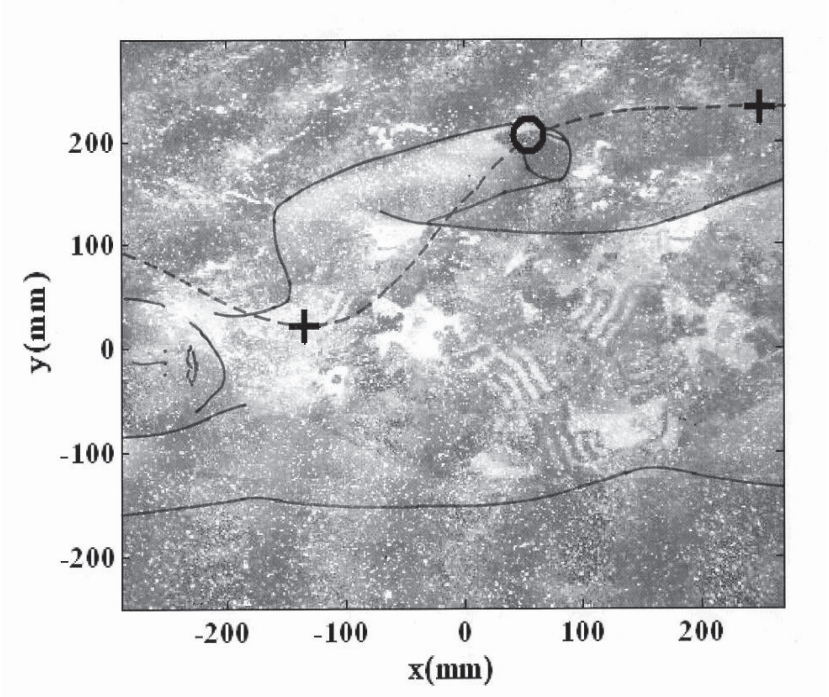

Fig. 2. Image of the swimmer as viewed from below. The outline of the swimmer is also depicted to clarify the posture. The open circle denotes the position of the tip of middle finger at this instant and the two cross marks the positions 1/15 s before and after this instant.

3. Particle image velocimetry

PIV is the most sophisticated method for measuring unsteady flow fields. In this method, a laser sheet illuminates tracer particles diffused in water. Two subsequent images of the particles are captured by a CCD camera and the path of the particle movement within a short interval is calculated. PIV has been frequently used to analyze the unsteady behavior of fish, insects and other creatures. For application of a flow field around a hand, it should be noted that the laser light must be intense as the flow field is not small.

3.1 Characteristic features

PIV is a global measurement technique used to trace a group of particles and determine their velocity through image processing. This technique has been developed owing to the rapid shortening in computer processing times, and is now widely used in the area of turbulence and heat transfer as a replacement for point measurements such as a hot-wire anemometry.

As will be mentioned in the next subsection, the principle is very simple: the velocity is taken as the moving distance devided by a short time interval. Since various global measurement techniques have been developed thus far, many researches using PIV have

been published and systems installed using PIV have become a commercial reality. The merits and demerits of the PIV are as follows:
Merits:

- It is non-disturbing owing to its contact-free setup.
- It has a fast response and can hence capture rapid changes of velocity and temperature.
- The instantaneous velocity, vorticity, and heat flux rates may be measured, as the velocity and temparature gradients can be measured instantaneously.
- Lagrangean measurements are possible including Lagrangean correlation and Lagrangean vector measurements.
- Without the movement of probes such as hot wires, the mean velocity and temperature are also easily obtainable.
- Multi-dimensional measurements are possible.

Demerits:

- Calibration is necessary.
- Tracer particles have to be diffused in water.
- The time resolution is poor.
- The dynamic range of the velocity is low.

3.2 Principle

Tracer particles diffused in water are illuminated by a laser sheet and an image is taken by a CCD camera. From two subsequential images within a certain small area at t_0 and $t_0 + \Delta t$ the correlation function is calculated by traversing the area in the searching region. The area that gives the maximum correlation is simply the one that includes particles corresponding to those at $t = t_0$ (see Fig.3). The moving distance of each particle $(\Delta x, \Delta y)$ is then determined. The velocity vector (u, v) in the two-dimensional plane is thus calculated by dividing the distance by the time interval Δt , i.e.,

$$u = \lim_{\Delta t \to 0} \frac{\Delta x}{\Delta t} \tag{1}$$

$$v = \lim_{\Delta t \to 0} \frac{\Delta y}{\Delta t} \tag{2}$$

Vorticity is a vector quantity that has three components and is a measure of the magnitude of fluid rotation. The concept of vorticity is important in the mechanism of an unsteady flow force. The simplest example for demonstrating vorticity is the lift force acting on an aerofoil. This force is generated by a starting vortex and a bound vortex around an aerofoil (see, for example, Lamb (1932) and Izumi and Kuwahara (1983)).
In this study we consider a two dimensional flow on a laser sheet. For this reason, only the z-component of the vorticity ζ is considered, which is simply defined as

$$\varsigma = \frac{\partial v}{\partial x} - \frac{\partial u}{\partial y} \tag{3}$$

The clockwise and anti-clockwise rotations of a fluid correspond to negative and positive values, respectively. The absolute value of ζ provides a measure of the rotation intensity.

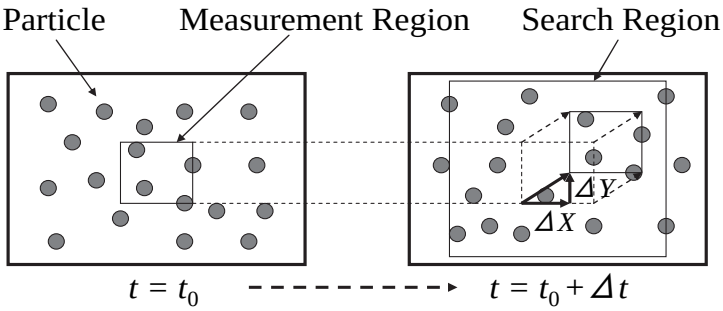

Fig. 3. Principle of determining velocity through PIV.

4. Motion analysis

Human movement constitutes of the superpositions of many rotating motions around a joint. In general, the motion of the center of gravity in human movement is not in a two-dimensional plane but in a three-dimensional space. Accordingly, the human body, in this case swimmer's hand, should be captured correctly as a function of time in a three-dimensional space.

To determine the coordinates in a three-dimensional space from video-recorded images, multiple images taken from video recordings in different directions relative to the subject are necessary. For this goal, we used a direct linear transformation (DLT) (Shapiro (1978), Abel-Aziz and Karana (1971)), which is used in the field of sports biomechanics. This DLT method has an advantage in the real positioning of cameras. Camera constants such as the direction of the optical axis and the focal length are not necessary to know. Instead the relationship between known coordinates in a real space and coordinates in a two-dimensional image is calibrated in advance. The relationships of several images, usually two images, determine the coordinates in a real three-dimensional space. The limitation of the optical axes are somewhat moderate. When two cameras are used, the angle between the two optical axes is about 30 to 150 deg. This method has been widely used in this respect.

5. Simultaneous measurement of hand motion and flow field

5.1 Synchronization between PIV and DLT

As shown in the previous section, PIV is a powerful method for visualizing the flow field around a swimmer, particularly around the hand. Considering the mechanism of propulsive force through hand movement, however, information on the precise formation and orientation of the hand is critical. PIV does not provide correct information on the hand motion. The DLT method, however, combined with high-speed cameras is useful for the determination of hand motion. However, correspondence of flow field by the hand motion and hence the force generation is still unclear. To determine the mechanism for the generation of propulsive force it is necessary to synchronize the DLT method with PIV. To know the instant when a force becomes strong and why the force is generated by the flow field, we have built a new system combining the two methods, which we call SMAP.

5.2 Separation of PIV and DLT in frequency range

PIV measurements are usually carried out in a dark room, with the use of only a laser light. On the other hand, the DLT method is usually applied under bright circumstances to digitize the position of the marker attached to the hand surface. To synchronize the two methods, the frequency range has to be separated into two ranges, one each for the PIV and DLT methods.

The remaining problem is how to synchronize the timing of the two measurements. We performed this operation using a pulse generator.

6. Experimental setup

We performed experiments using a flume installed at the University of Tsukuba (Igarashi Industrial Works Co., Ltd.). The test section is 4.6 m long, 2 m wide, and 1.5 m high with a 1.2 m water depth. It can provide a maximum flow of 2.5 m/s. The flow speed was set at 1.0 m/s.

6.1 Subject

The subject is a male triathlete of the Univesity of Tsukuba volunteered for the present purpose. We explained the aim, procedure and the risk, and got his approval to the cooperation.

6.2 Method

We used an Nd-YAG laser with a sufficiently high intensity (Solo PIV 120; New Wave Research Inc.). Under the flume a CCD camera (ES1.0, Eastman Kodak Co.) for PIV was set. This camera captures the images reflected by a mirror (see Fig. 4). Two high-speed cameras (FASTCAM-512PCI, Photron) for DLT were set as shown in Fig. 4. We paid attention only to the swimmer's right hand for the present experiment. The subject wore glasses for protection against the strong laser light and also a black globe made from silicon rubber to avoid halation. The tracer particles and data aquisition procedure were quite simiar to those in previous experiments (Matsuuchi et al. (2009)).

During the motion analysis, we captured 1088 frames at one time. We digitized images from the video using 2D and 3D video analysis software (Frame DIAS version 3, DKH Co., Ltd), and determined the traces of the hand, the velocity and the geometry of the palm. The points digitized are the metacarpopharangeal joints of the second and fifth fingers and the tip of the third finger. Fig. 5 shows the points and a local coordinate system (X, Y, Z) fixed to the palm. The coordinates are related to the global coordinates (x, y, z) fixed to the flume. As will be explained later, x is the flow direction; y the horizontal backward direction; and z vertically upward. The global coordinates (x, y, z) were measured directly by the CCD cameras, and the local coordinates (X, Y, Z) of the specified three points of the palm were calculated. The identification of these palm points gives the geometrical configuration of the palm. On the other hand, in the PIV measurements 128 images, or 64 pairs, were taken. Each pair taken at 1 ms interval represents a set of two kinds of fields - velocity and vorticity fields. In the PIV measurements the relationship between the real coordinates and two-dimensional image data needs to be determined in advance. Calibrations were carried out for this purpose.

To determine the global coordinates (x, y, z) from the two-dimensional data captured by CCD cameras, it is necessary to obtain in advance the relationship between the coordinates (x, y, z) and the two-dimensional image data through a calibration procedure.

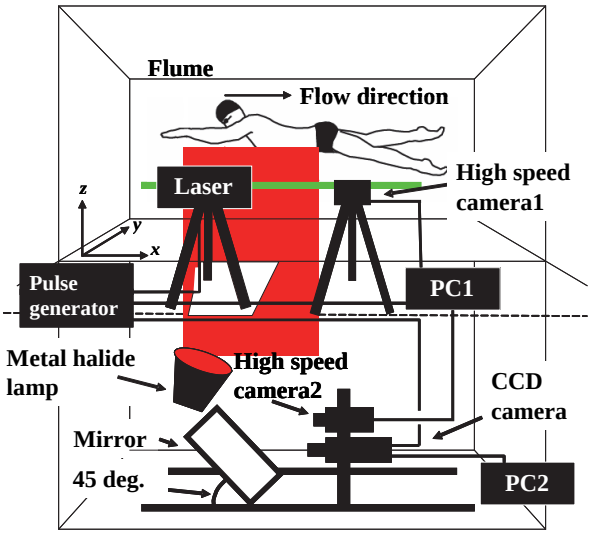

Fig. 4. Experimental configuration and setup.

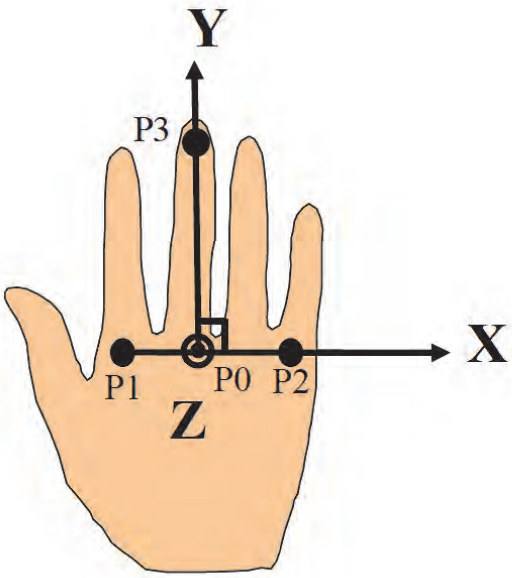

Fig. 5. Local coordinates fixed on the palm.

To combine the two methods we used two kinds of light with different spectrum characteristics. One is an Nd-YAG laser, and the other the light of a metal halide lamp. The metal halide lamp was covered with a red film for the DLT. For this method, band-pass filters that pass through a light at a wavelength of 640 to 700 nm are attached to the front of the lens of the CCD cameras for DLT method. On the other hand, for PIV a band-pass filter ranging between 532+2 and 532-2 nm was used. The wavelength of 532 nm corresponds to that of the Nd-YAG laser. The ranges of the wavelength utilized for the two methods are illustrated in Fig. 6. The first wavelength was used for PIV and was created using a line band-pass filter, whereas the second wavelength was created using a red band-pass filter and was used for the DLT method.

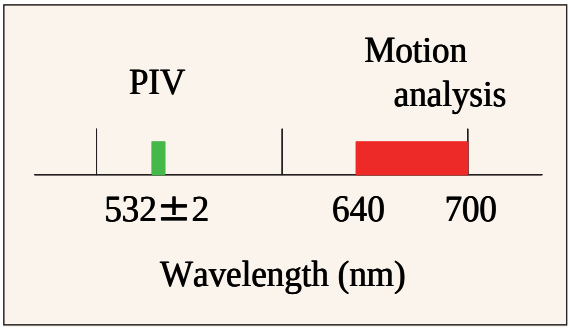

Fig. 6. Separation of ranges of wavelength - for PIV and for motion analysis.

The timing was synchronized with pulses generated by a pulse generator. Our PIV system is capable of capturing images at a minimum of every 1/15 of a second, whereas the high-speed cameras are able to take photos within shorter periods. To synchronize two signals, we chose Δt= 0.068 s for PIV, while setting the period at 0.004 s for the DLT. A timing chart is shown in Fig. 7.

As mentioned before, two subsequent images taken within a short interval determine the velocity field. The timing is also controlled by two pulses, Pulse 1 and Pulse 2, generated by the pulse generator. The interval of the two pulses was set at 1 ms in the experiments.

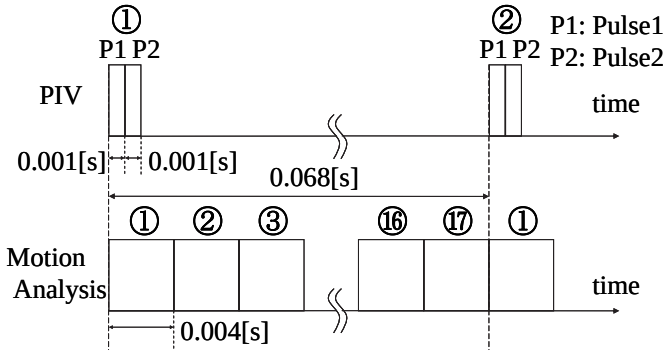

Fig. 7. Timing chart of the dual analysis system. The time interval used for obtaining the flow field using PIV was set at 68 ms, while the motion analysis using high-speed cameras set at 4 ms.

7. Results

Our SMAP system can be used to determine the flow field and hand movement of a swimmer simultaneously using geometrical configurations. It is a start of thinking of the mechanism of propulsive force generation in swimming. This mechanism will be discussed in terms of the unsteady properties of the flow field and hand motions. The results teach us many things about the mechanism of how vortices are created and how the momentum leading to thrust force is generated. While this mechanism is very complex, it is quite interesting although a high-level of knowledge on fluid mechanics is needed for proper understanding.

7.1 Motion analysis

First, we show the the changes of hand orientation in a three-dimensional space. Our system determines the variations of hand orientation accurately, as shown in Fig. 8. The thick lines corresponds to the instants at which the PIV determines the velocity and vorticity fields, i.e., t = 0.036, 0.104, and 0.172 s. The initial time t = 0 chosen arbitrarily is different for each event. A complex change in the hand path can be easily seen, which makes it difficult to interpret its role in force generation.

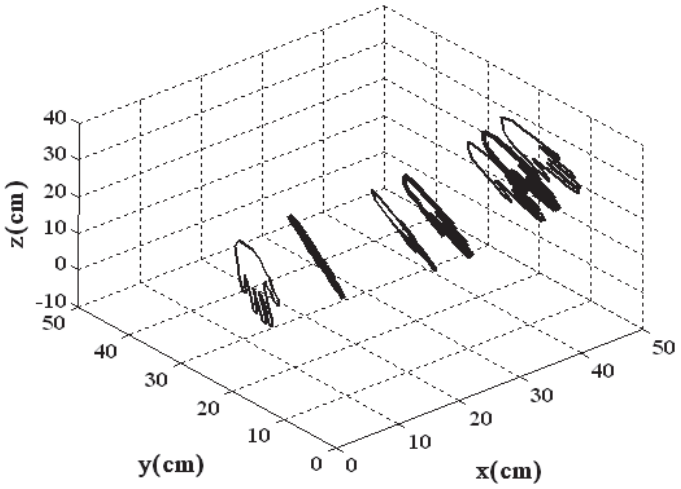

Fig. 8. Three-dimensional path of hand and the variations in the palm orientation. Rapid changes of the hand path and orientation can be seen.

While our motion analysis system can be used to determine the coordinates of the palm in a three dimensional space, the interpretation of the unsteady mechanism of force generation in a three-dimensional space is very complex and difficult to understand. Therefore, in this report, only a two dimensional field in a laser sheet is discussed for simplicity. A hand path in the transition phase from in-sweep to out-sweep and the definition of the angle are shown in Fig. 9. During this phase, it is plausible that a significant generation of momentum can be produced. The pitch angle, which is the flow direction measured from the normal to

the palm, was chosen as an important parameter to determine the circulation of the palm. It was noted that if we view the palm as an aerofoil, the leading edge changes from the thumb side to the fifth finger side. This indicates that a change in the sign of the circulaltion around the palm occurs (see Prandtl and Tiejens (1934) for further details). This change is important to determine the generation of forces that occur from vortex motions (see Matsuuchi et al., 2009). The change of the leading edge durintg the phase is a critical difference in the generation of unsteady forces created from flight or locomotion in insects and birds.

Real variations of the palm projected on the horizontal x-y plane are shown in Fig. 10. Variations of the flow direction relative to the hand are crucial for understanding of the generation of vortices and thus the production of force. Time variations of the hand velocity and pitch angle measured in the frame relative to water are illustrated in Fig. 11. The thick vertical lines correspond to the instants at which PIV measurements were made, i.e., at t = 0.036, 0.104, and 0.172 s. During the period from t = 0.104 to 0.172 s, the velocity is decreased by about 1 m/s and the pitch angles vary largely. The magnitude of the angle variation is as large as 120 deg. This is simply the transition phase in the hand stroke from an in-sweep to an out-sweep. These variations of hand velocity and pitch angle are essential during the transition phase in the crawl stroke. We now calculate rotational velocity compared to the uniform velocity, which is usually called the reduced frequency. If this rate is small, the flow is considered to be steady. If we set the chord length as 10 cm, the reduced frequency is calculated as 3.1. This value is too high to neglect the unsteadiness.

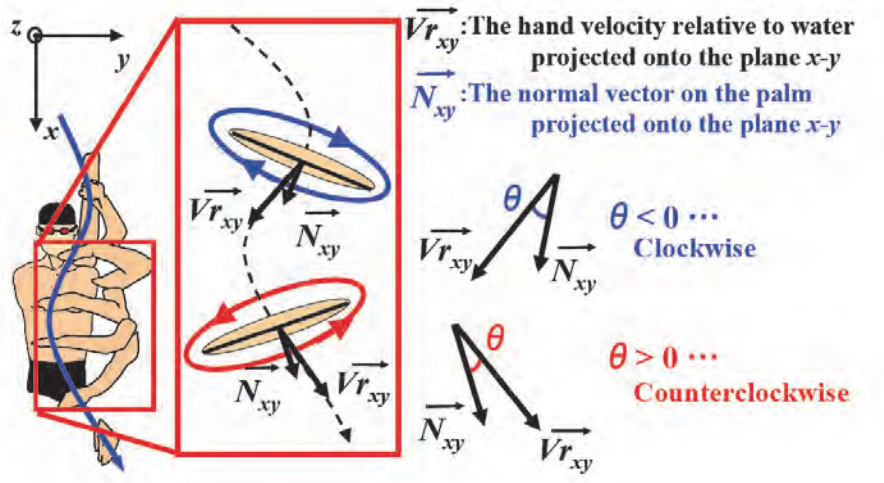

Fig. 9. Definition of and change in the angle of pitch along the hand path.

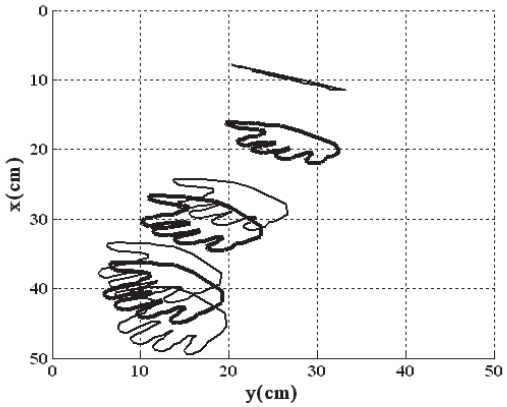

Fig. 10. Temporal variations of hand configuration in the *x-y* plane. The thick lines correspond to the instants at 0.036, 0.104, and 0.172 s. The corresponding configurations at other instants are also superposed using thin lines to facilitate an understanding of the variations in the characteristics of a hand motion.

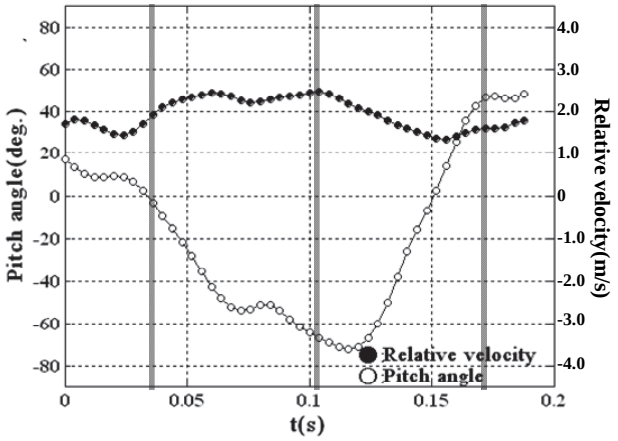

Fig. 11. Variations of pitch angle and hand velocity. The three vertical lines drawn in bold indicate instants of 0.036, 0.104, and 0.172 s

Thus far, the hand paths have been drawn in a three-dimensional space fixed to the flume. However, the real swimming is performed in still water. In this meaning, it seems to be better to depict the path relative to the running water. The palm paths in the *x-y* and *x-z* planes of the transformed coordinates of still water are picked up and shown in Figs. 12 (a) and (b), respectively. In the figure, the green colored palms correspond to those at the instant PIV works. The vectors in red denote the movement direction, while the vectors in blue are unit normals to the palm. A red vector of 3 m/s is also drawn in the corner as a reference. Remarkable and rapid changes of the palm orientation can clearly be seen from these figures.

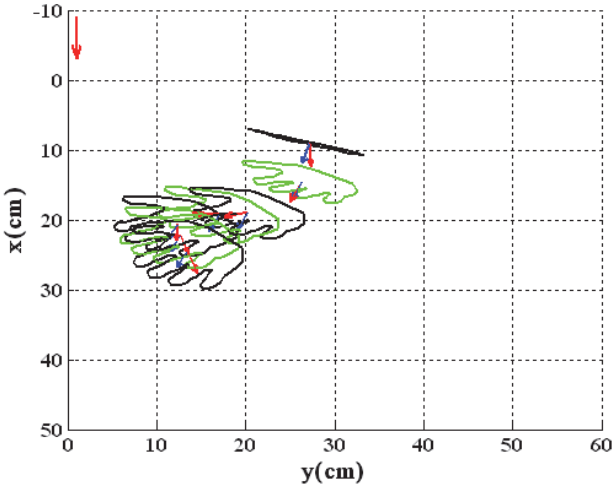

(a)

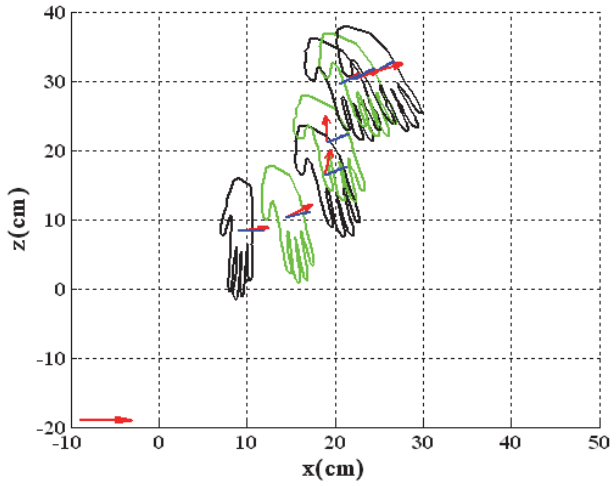

(b)

Fig. 12. Palm outlines relative to water are depicted. The red arrows denote the velocity of the palm relative to the water. The subject moves his hand in a complex manner, and rapidly changes the orientation in both planes.

7.2 Visualization of flow field

In Fig. 13, first we show a hand position and body viewed from the bottom at 0.036 s. Note here that although it appears to be the left arm owing to mirror imaging, the arm shown in the figure is actually the right one. The hand position relative to the aswimmer's trunk can easily be seen. The velocity and vorticity fields corrresponding to those at the instant

depicted in Fig. 13 are shown in Figs. 14(a) and (b), respectively. To clarify the generation of velocity fluctuations from the hand movement the mean velocity was subtracted from the real velocity vectors. At this stage, no remarkable increments in velocity or no strong generation of momentum occured. Only a weak positive rotation, shown in white, can be seen near the little finger.

Velocity and vorticity fields at an instant 0.068 s later are depicted in Fig. 15. The positive rotation that appeared in the previous instant shown in Fig. 14 remains in the place where it existed at the previous instant. More intense rotations of positive and negative signs are found to be produced adjacent to the hand. It can be seen that the generation of momentum in the positive x-direction can be detected between two vortices; the positive vortex produced at the previous instant and a newly produced negative rotation. Such momentum generation simply corresponds to the production of force, which is a reduction from Newton's second law of motion. A similar but simple circumstance occurs when an aerofoil is suddenly started (Lamb (1932)). In Fig. 16 the velocity field obtained at t = 0.172 s through PIV is shown as a solid line and hand positions at two other instants, t = 0.036 and 0.104 s are shown as broken lines. The generation of momentum in the positive x-direction can be clearly seen in the figure. Note that this direction is opposite to the negative x-direction, which is the swimming direction. The generation of momentum is the result of a pair of vortices rotating in opposite directions. Such momentum generation leads to a thrust force by the hand, which is indeed a consequence of Newton's second law of motion, as already explained.

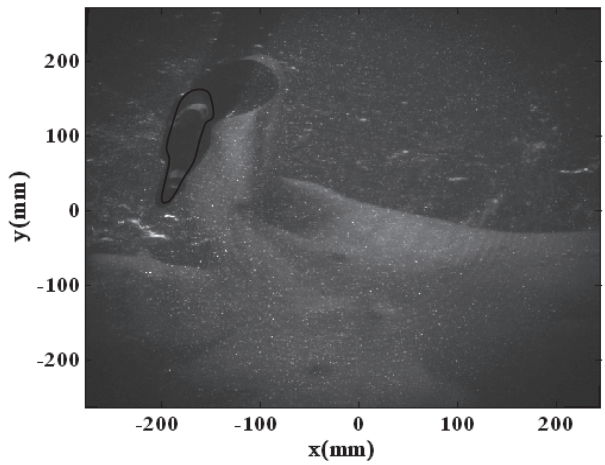

Fig. 13. Swimmer viewed from below at 0.036 s. The closed curve in the solid line indicates the near side of the palm on the laser sheet.

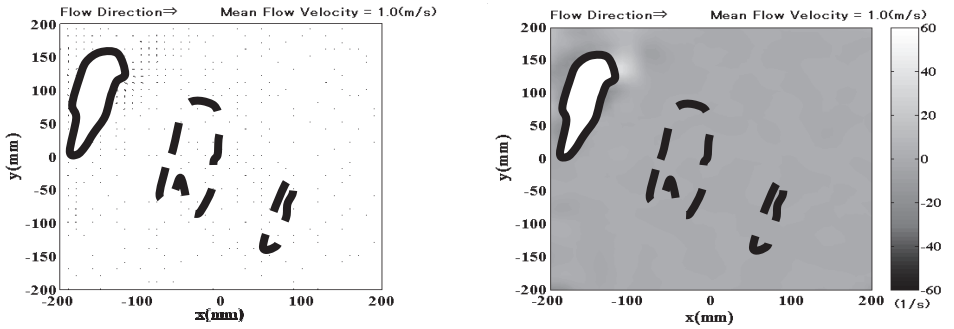

Fig. 14. Velocity (a) and vorticity (b) fields at 0.036 s are shown. The solid line corresponds to the outline of the hand at this instant and the other two broken lines show the outlines at instants 0.068 s and 0.136 s later.

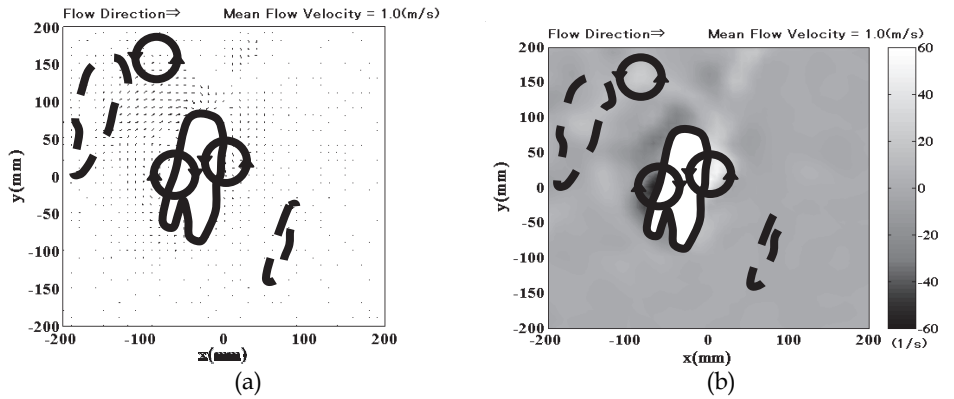

Fig. 15. Velocity (a) and vorticity (b) fields in the *x*-*y* plane at 0.104 s. The solid line corresponds to the outline of the hand cross section at this instant and the two broken lines show the outlines at 0.036 s and 0.172 s. The three circles with arrows indicate the vortices.

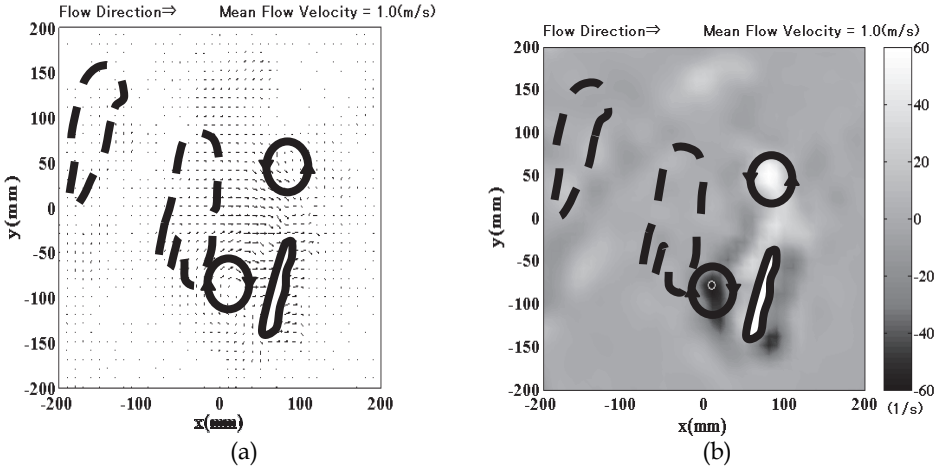

Fig. 16. Velocity (a) and vorticity (b) fields in the *x*-*y* plane at the instant 0.172 s. The solid line is an outline of the cross section at this instant, and the two broken lines are those at 0.036 and 0.104 s. The two circles with arrows indicate vortices generating momentum in the positive *x*-direction.

8. Discussions

Our main concern is to find the source of propulsive force arising from hand movements. To obtain a better understanding of the source, a synchronized system for the visualization of flow fields and hand motions was established.

The orientation of the palm was found to vary in a complex manner. When hand orientation changes rapidly, vortex generation and shedding, and consequently momentum generation are found to occur in the flow field. Such a vortex behavior makes the flow fields unsteady. The introduction of unsteadiness in the generation of propulsive force while swimming is a newly developed idea. Thus far, an approach for understanding the mechanism of propulsive force has been developed in many researches on the basis of the concept that the motions of the hand and foot seem to be steady. This approach is called the quasi-steady theory. Several authors have pointed out that quasi-steady results lead to an underestimation of force magnitude (Sanders (1999), Toussaint, Van den Berg and Beek (2002)). The results of the present research will provide important information on the momentum generation and force production due to the flow unsteadiness.

However, some problems remain. The most serious one is the limitation of the sampling time when using PIV. The movement of a human swimmer is not too slow, but our sampling interval is only 66 ms at minimum. Therefore, it is difficult to trace the details of a flow field. While there is a way to overcome this difficulty, it is not easy to implement owing to the high costs involved. The other problem is the limitation of the obserbvation area, i.e., observations using a laser are essentially limited to only the area within the laser sheet, i.e., they are two dimensional observations. Observational data accumulated in many horizontal planes could provide sufficeint information. However, if we could make experiments simultaneously in many horizontal planes, the task were not tolerable to make.

Before concluding this section, we will now introduce a new approach called stereoscopic PIV (see Prasad and Adrian (1993), Prasad and Jensen (1995), in addition, for the case of turning fish, see Sakakibara et al.(2004)). This technique can be used to reconstruct a quasi three-dimensional flow field.

Fig. 17 shows the results obtained through stereoscopic PIV are shown. The subject is an elite short-distance swimmer from Japan, who swam in the flume at a velocity of 1.0 m/s. The laser sheet is placed in a vertical plane normal to the swimming direction. The figure shows the velocity field in the y-z plane, or in a vertical plane. The first picture in Fig. 17(a) shows a photo taken obliquely behind the subject, while the right image is the flow field at the initial instant t = 0. The color bar represents the magnitude of the velocity component in the x-direction, i.e., the direction opposite to the swimming one. The vectors are the velocity vectors in the y-z plane. The instant t = 0 is the moment when the hand passes through the laser sheet. In this stage the velocity component in the flow direction induced from the hand motion appears to be slight.

At the next instant, t = 0.067 s (b), when the hand passes away from the laser, the area of strong axial velocity (in the x-direction) increases. This means that the momentum increases together with a strong clockwise rotation leading to the propulsive force. At the instant t = 0.134 s (c) an area with a strong rotation flows downstream and a weak area remains there.

In the above three stages were picked up. If we could obtain sequential velocility fields at a shorter time intervals, it would be possible to reconstruct three-dimensional velocity or vorticity fields by applying Taylor's frozen-flow hypothesis. We will be able to obtain important information from the three-dimensional structure of vortices and velocities induced by hand movement. This three-dimensional data is expected to give a definitive answer to the problems for the generation mechanism and time variations of a propulsive force.

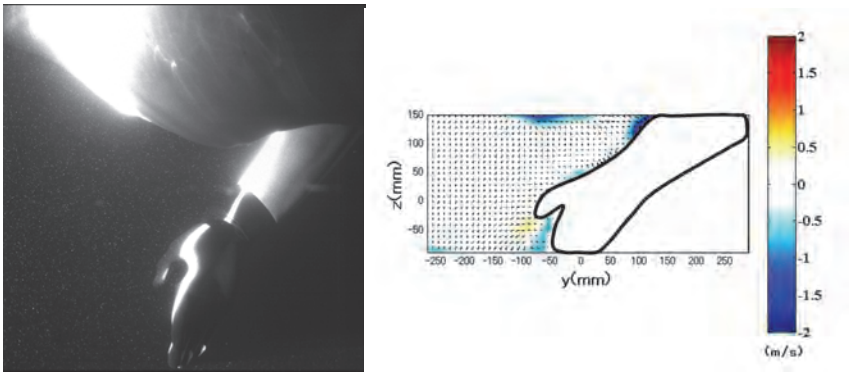

(a) t=0.0 (s)

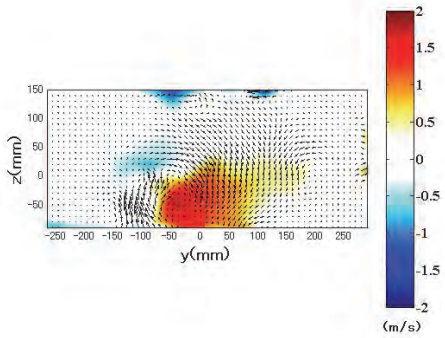

(b) t=0.067 (s)

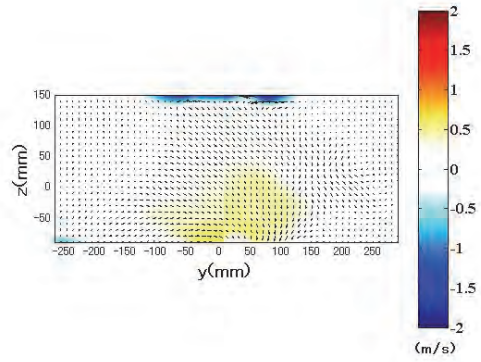

(c) t=0.134 (s)

Fig. 17. Flow field in the y-z plane obtained through the stereoscopic PIV method. The vectors denote the velocities in the plane, while the colors represent the magnitude induced by the hand motion opposite to the swimming direction, i.e., the x-direction.

9. Concluding remarks

Our system SMAP method can provide us with significant information for understanding the mechanism of force. This system can be used to quantitatively evaluate an unsteadiness such as a reduced frequency and from the flow field we can determine the instants of large momentum and hence the produced propulsive force of significant magnitude.
In most cases, however, our data is still limited to that obtained from two-dimensional information. To adopt the present approach for real swimming and traiming routines, many more experiments need to be carried out and much more information is required.
Our system, which combines two different methods, has room for modification. Three dimensionality and a shorter acquisition are included in the new system. Such a modified system is expected to provide us knowledge useful for improving swimming techniques and to become a powerful tool for refining or reforming efficient swimming form.

10. Acknowledgements

This study was supported by a Grant-in-Aid for Scientific Research ((B)21300228) from the Japan Society for the Promotion of Science.

11. References

Abdel-Aziz, Y.I., Karana, H. M. (1971). Direct Linear Transformation from Comparator Coordinates into Object Space in Close-range Photogrammetry. ASP Symposium on Close-Range Photogrammetry, American Society of Photogrammetry, Falls Church

Arelllano, R. (1999). Vortices and Propulsion. In: Applied Proceedings of the XVII International Symposium on Biomechanics in Sports, 53-66

Arelllano, R., Pardillo, S., Gavilan, S. (2002). Underwater Undulatory Swimming: Kinematic Characteristics, Vortex Generation and Application during the Start, Turn and Swimming Strokes. In: Proceedings of the XXth International Symposium on Biomechanics in Sports, Universidad de Granada

Berger, M.A.M., de Groot, G., Hollander, A. P. (1995). Hydrodynamic Drag/Lift Forces on Human Hand/Arm Models, *Journal of Biomechanics*, 28, 125-133

Bisplinghoff, R. L., Ashley, H., Halfman, R.L. (1955). *Aeroelasticity*, Chap. 5, Addison-Wesley Pub.

Bixler, B., Riewald, S. (2002). Analysis of a Swimmer's Hand and Arm in Steady Flow Conditions Using Computational Fluid Dynamics, *Journal of Biomechanics* 28, 125-133

Colwin, C.M. (2002). *Breakthrough Swimming*, Chap.5, Human Kinetics

Counsilman, J.E. (1971). The Application of Bernoulli's Principle to Human Propulsion in Water, *Swimming* 1, Eds. Lewillie, L. and Clarys , J.P., University Park Press, 59-71

Dickinson, M. (1996). Unsteady Mechanisms of Force Generation in Aquatic and Aerial Locomotion, American Zoologist, 36, 537-554

Izumi, K., Kuwahara, K. (1983). Unsteady Flow Field, Lift and Drag Measurements of Impulsively Started Elliptic Cylinder and Circular-Arc Airfoil, *AIAA*-83-1711

Lamb, H. (1932). *Hydrodynamics*, 6th Ed., Art. 157, Cambridge Univ. Press

Matsuuchi, K., Miwa, T., Nomura, T., Sakakibara, J., Shintani, H., Ungerechts, B.E. (2004). Unsteady Flow Measurement around a Human Hand in Swimming Using PIV, *9th Annual Congress of the ECSS*, CDROM.

Matsuuchi, K., Miwa, T., Nomura, T., Sakakibara, J., Shintani, H., Ungerechts, B.E. (2009). Unsteady Flow Field around a Human Hand and Propulsive Force in Swimming, *Journal of Biomechanics*, 42, 42-47

Prandtl, L., Tiejens, O. G. (1934). *Applied Hydro- and Aeromechanics*, Chap. 6, Dover Pub.

Prasad, A. K., and Adrian, R. J. (1993). Stereoscopic Particle Image Velocimetry Applied to Liquid Flows, *Experiments in Fluids*, 15, 49-60

Prasad, A.K., Jensen, K. (1995). Scheimpflug Stereocamera for Particle Image Velocimetry in Liquid Flows, *Applied Optics*, 34, 7092-7099

Sakakibara, J., Nakagawa, M., Yoshida, M. (2004). Stereo-PIV Study of Flow around a Maneuvering Fish, *Experiments in Fluids*, 36, 282-293

Sanders, R. H. (1999). Hydrodynamic Characteristics of a Swimmer's Hand, *Journal of Applied Biomechanics*, 15, 3-26

Schleihauf, R. E. (1979). A Hydrodynamic Analysis of Swimming Propulsion, *Swimming III*, 70-109

Shapiro, R. (1978). The Direct Linear Transformation Method for Three-Dimensional Cinematography, *Research Quarterly*, 49, 197-205

Toussaint, H. M., Van den Berg, C., Beek, W.J. (2002). ``Pumped-Up Propulsion" during Front Crawl Swimming. *Medicine and Science in Sports and Exercise*, 34, 314-319

Ungerechts, B. E. (1981). Propulsive Principle of Fast Swimming Vertebrates Analysed by Flow Visualizing Techniques, In: Abstracts of the VIIIth International Congress of Biomechanics, Nagoya, Japan, 165

Ungerechts, B.E. (1992). The Interrelationship of Hydrodynamical Forces and Swimming Speed in Breaststroke. In: D. MacLaren, T. Reilly & A. Lees (eds.), *Biomechanics and Medicine in Swimming -Swimming Science* VI. E. & FN Spon, London, 69-73